An Extended Finite Element Method Study on the Effect of Reinforcing Particles on the Fatigue Crack Propagation Behavior of Functionally Graded Plates

Ehsan Naderi [1], Mohsen Taghizadeh[1*], Yadollah. Alinia[1]

[1] Mechanical Engineering Department, Hakim Sabzevari University, Sabzevar, Iran.
* The corresponding author: m.taghizadeh@hsu.ac.ir.

Abstract:

In this work, it is looked into how adding silicon nitride (Si_3N_4) particles into Functionally Graded Material (FGM) plates affects their resistance to fracture propagation. A comprehensive numerical study is performed using the extended finite element method (XFEM) implemented in the Abaqus software to investigate the impacts of different Si_3N_4 particle characteristics, including geometry, size, and volume percentage, on the fatigue behavior of FGM plates. The results indicate that these variables have a significant influence on the fracture formation rate and overall fatigue life of the FGM. Specifically, square Si_3N_4 particles displayed higher efficiency in arresting crack development compared to alternative shapes, which was attributable to their optimal stress distribution. Results show that adding 10, 20, and 30 weight percent of square Si_3N_4 particles with a side length of 0.89 μm to the FGM increased the fatigue life by 70.47, 57.69, and 53.79 percent, respectively, compared to the case without reinforcing particles. Furthermore, increasing the volume percentage of Si_3N_4 particles while concurrently reducing their size resulted in a significant gain in both fatigue life and overall strength of the FGM plates. These findings highlight the potential of Si_3N_4-reinforced FGMs as a highly effective method for reducing fatigue-induced damage and increasing the service life of engineering components. The findings of this study provide useful insights for the design and optimization of FGM-based structures under cyclic loading conditions.

Keywords:

Fatigue failure, functionally graded materials, extended finite element method, crack propagation, fatigue life

1. Introduction

Rapid advances in technology have made the development of materials with exceptional mechanical and thermal properties necessary, particularly in delicate fields like microelectronics and aerospace. Researchers have been looking at new materials with complex structures and variable characteristics in response to these needs. By integrating the various qualities of multiple components, FGMs, one such growing class of materials, provide a unique solution. The concept of FGM was initially presented during Japanese space programs in the 1980s. Parts that could withstand severe temperature fluctuations were the aim of study. The primary objective was to develop a material that could shift from being a durable metal surface to a heat-proof ceramic surface. This new approach allowed for the creation of parts with great mechanical strength that can withstand high temperatures for extended periods. FGM is commonly practiced in many fields and has gained significant scholarly interest in recent times because of its varied manifestations and evolving characteristics. These materials constitute a new generation of composites in which mechanical parameters including Young's modulus, Poisson's ratio, and shear modulus vary continuously and gradually throughout the material. This unique quality allows for the creation of components that have an optimal distribution of stress and enhanced performance. In other words, the mechanical properties of FGMs change gradually depending on specific application requirements, as opposed to staying consistent across the entire material. Unlike traditional composites made up of separate layers of materials, FGMs exhibit property change on a microscopic scale. This distinguishing property makes FGMs an excellent alternative for applications that need a graded distribution of attributes. In essence, by progressively adjusting the ratio of constituent components, desirable qualities may be adjusted in various parts of the material. FGMs exhibit greater structural strength than layered composites because they have a continuous distribution of properties on a microscopic scale. This integrity decreases the chance of cracks starting and spreading at interfaces, enhancing resistance to fatigue. Yet, their graded structures make them prone to fracturing when subjected to cyclic loading. In numerous practical situations, repetitive loads can rapidly propagate small cracks leading to unforeseen breakdowns. Therefore, it is important to

accurately assess how cracks behave and predict the lifespan due to fatigue when developing components made from FGMs. Using numerical simulations to study crack propagation in FGMs has become crucial for improving our knowledge of failure processes and advancing the progress of these cutting-edge materials. Recently, numerical simulations have emerged as an effective method for analyzing the fatigue characteristics of FGMs in depth. Using these techniques, scientists aim to gain a more profound insight into the intricate processes that control the initiation and growth of cracks in these substances. Singh et al. [1] and Bhattacharya et al. [2] have used the finite element method (FEM) to model crack behavior in FGM plates with discontinuities. These studies have shown that the stress intensity factor (SIF) and fatigue life of these materials are greatly affected by the location, type, and density of cracks and discontinuities. Wang et al. [3] showed that adding silica nanoparticles to an epoxy matrix improves the mechanical characteristics of these composite materials. Nevertheless, an excess number of nanoparticles may result in a decrease in strength. Using FEM, Bhattacharya and Sharma [4], modeled the fatigue performance of FGMs exposed to thermal loading and investigated the influence of discontinuities on their fatigue life. According to their studies, it was discovered that the ceramic components in FGMs are less resistant to crack propagation. By utilizing numerical simulations with Abaqus software, Zakari and Jafari [5], analyzed the stress intensity factors of both plain and reinforced isogrid plates. Their results indicated that reinforcements and geometric variations such as crack length and angle have a significant impact on stress distribution and stress intensity factors in reinforced plates. Bartaula et al. [6] studied the accuracy of XFEM in predicting fatigue crack propagation in compact tension (CT) specimens and pipelines. Their research demonstrated that when XFEM is paired with appropriate methods, it can forecast the fatigue life of pipeline structures. Bhattacharya et al. [7] studied the expansion of fatigue cracks in a bi-layered FGM using an extended finite element technique. The researcher studied the effects of exponential variations in material characteristics, as well as simultaneous thermal and mechanical stresses, on the longevity of components and stress intensity factor. Bharti et al. [8] carried out research on the uses of FGMs reinforced with carbon nanotubes (CNTs). Their results suggest that CNT-enhanced FGMs could be used in magnetic resonance imaging (MRI) cryogenic tubes, automotive combustion chambers, rocket nozzles, and solar panels. Anari and

Salehi [9] simulated the crack initiation and growth in a functionally graded dental implant under cyclic axial loading. The research utilized the Mori-Tanaka model to investigate material gradation, developed a Fortran program to describe FGM in Abaqus, and employed an XFEM to analyze crack propagation. Their findings indicated that FGM implants with a power-law index lower than one demonstrated enhanced resistance to crack propagation under cyclic loading conditions. Shedbale and et al. [10] examined the linear and nonlinear characteristics of a cracked plate with random discontinuities through the FEM. During cyclic loading tests, researchers looked into how yield stress affects fatigue life. The evaluation used the von Mises failure criterion, Ramberg-Osgood material behavior model, and Paris' equation. Singh et al. [11] researched the propagation of cracks in a hydroxyapatite-titanium plate with a gradient in the Y direction, considering the impact of dislocations. A particular FEM was employed in Abaqus to demonstrate the impact of the loading method, FGM composition, and gradient on the crack trajectory. Zaidi et al. [12] performed a comparison of different modeling techniques for FGMs. Their findings showed that the self-consistent grading method is more effective than other methods because it is highly accurate and easy to use. Furthermore, the effect of incorporating silica nanoparticles on the mechanical characteristics of polymer composites was examined by Diyar Kaka et al. [13]. According to their findings, the elasticity modulus increased and the ductility decreased as the concentration of silica nanoparticles decreased. Ulukoy et al. [14] investigated the fatigue crack behavior of a functionally graded cylindrical material made of aluminum alloy 2014 reinforced with silicon carbide (SiC) particles. They tested samples with three different notch types (center, single-edge on SiC-rich side, and single-edge on aluminum-rich side) under tensile cyclic loading and showed that the SiC distribution has a significant effect on the initiation and propagation of fatigue cracks. Their results showed that increasing the SiC ratio leads to an increase in fatigue life, a delay in crack initiation, and an improvement in crack growth resistance. Xu et al. [15] investigated the fatigue crack growth behavior in a Functionally Graded Metal Matrix Composite (FGMMC) consisting of SiC particles reinforced with Al matrix. The results showed that the fatigue crack growth rate increases with increasing stress ratio, which can be explained by the crack closure mechanism. Also, a decrease in crack growth was observed during crack propagation from SiC layers with low volume

fraction to SiC layers with high volume fraction. Furthermore, crack deflection and branching at the interfaces were observed, which reduced the fatigue crack growth rate. Sources and related content. Bhattacharya et al. [16] designed, synthesized, and characterized two types of multilayered FGMs, namely aluminum-silicon carbide (Al/SiC) and nickel-alumina (Ni/Al_2O_3), with varying ceramic volume fractions. Three key properties, including effective flexural strength, thermal fatigue behavior, and thermal shock resistance, were evaluated to characterize the FGMs. The results demonstrated that increasing the number of layers led to a progressive improvement in the performance of the FGMs. Xu et al. [17] investigated the fatigue crack growth properties of homogeneous and graded SiC particulate-reinforced aluminum composites using three-point bending fatigue testing. The results showed that the fatigue crack growth rate increases with increasing SiC particulate volume fraction in the homogeneous composites. However, the graded composite exhibited better fatigue crack growth resistance than the homogeneous composites. They observed that crack deflection and branching occurred at the transition region between the 5% SiC and 15% SiC layers in the graded composite, which led to a decrease in the fatigue crack growth rate. Agrawal et al. [18] investigated the fatigue crack growth behavior and life prediction of Si_3N_4/TiB_2-reinforced hybrid metal matrix composites (HMMCs). They found that adding 6 wt% TiB_2 to the AA7075 composite improved fatigue life and fracture toughness. They also proposed an exponential model for predicting the fatigue life of HMMCs, which showed good agreement with experimental data. Lal et al. [19] investigate the mixed-mode stress intensity factor (MMSIF) analysis in cracked FGM plates with different material distribution models using the XFEM. The primary objective of this study is to evaluate the mean and variance of MMSIF with crack growth and probability of failure analysis (PFA) of edge-cracked FGM plates under various loading conditions. This evaluation is conducted utilizing XFEM in conjunction with the Second-order Perturbation Technique (SOPT). The simulated results are then compared with published results to validate the efficacy of the user-defined MATLAB code. Lai et al. [20] investigated the fatigue crack growth behavior and life prediction of Si_3N_4/TiB_2-reinforced hybrid metal matrix composites. They found that adding 6 wt% TiB_2 to the AA7075 composite improved fatigue life and fracture toughness. They also proposed an exponential model for predicting the fatigue life of HMMCs, which showed good

agreement with experimental data. Chiu et al. [21] investigated the deformation, interfacial behavior, and particle damage in magnesium-partially stabilized zirconia (Mg-PSZ) particle-reinforced transformation-induced plasticity (TRIP) steel composites using scanning electron microscope (SEM) in-situ tensile tests and finite element simulations. In this study, simulation models employing an elastic model for ceramic particles and a Johnson-Cook plastic model for the matrix were utilized to compare the performance of various interface models (perfect, cohesive zone model (CZM), and combined CZM/ XFEM). The results demonstrated good agreement between the simulations and experimental results, with a relative error in crack length of only 4.6%. Furthermore, debonding angle analysis revealed that particle geometries with sharp edges accelerate damage initiation. Mosayyebi et al. [22] numerically investigated the effect of using composite patches with different geometric shapes to improve the fatigue life of cracked aluminum alloy panels AA7075-T6 and AA2024-T3 and compared them with the available experimental results. The CZM and the XFEM were used for static and fatigue analyzes. Four types of rectangular, trapezoidal, left-oriented triangular and right-oriented triangular composite patches were used in the numerical analysis. By combining XFEM and CZM methods and using the Paris equation, fatigue crack propagation and fatigue life of cracked aluminum panels were logically predicted. A composite patch with proper shape and geometry can significantly improve the fatigue life of the repaired panel. With a 204% improvement in fatigue life compared to the unrepaired panel, the repaired sample made of AA2024-T3 aluminum alloy achieved the most significant improvement in fatigue life. In AA7075-T6 alloy samples repaired with composite patches, the samples repaired with rectangular and trapezoidal patches experienced the highest fatigue life increases, respectively with 342% and 290% compared to the unrepaired samples. The comparison of numerical simulation results with the available experimental results shows a good agreement. Bouchlarhem et al. [23] numerically investigated the influence of material grading on the fracture path in ceramic/metal FGMs. The finite element method was used to model the crack growth path, and two types of ceramic/metal FGMs were considered to examine the effect of material grading on the fracture path. The results showed that the difference in crack growth path can be attributed to the influence of the material gradient. Additionally, it was found that the easiest way for crack propagation is when the

crack is perpendicular to the material grading. A crack located on the stiff side of the specimen exhibits less deviation compared to a crack on the soft side. Karci et al. [24] investigated the fatigue crack growth rate and propagation mechanisms in SiC particle-reinforced aluminum alloy matrix composites. This research was conducted experimentally, and composites reinforced with 5, 10, and 15 volume percentages of SiCp and unreinforced 2124 aluminum alloy billets were produced using the powder metallurgy (PM) production technique. The results were analyzed comparatively. Optical microscope results to determine the microstructural properties of the billet and samples showed that although SiC particles were rarely clustered in the Al alloy matrix, they were generally homogeneously dispersed. Fatigue crack propagation rates were determined experimentally. While the highest crack initiation resistance was achieved at 5% SiC volume ratio, the slowest crack propagation rate in the stable crack propagation region was found in the unreinforced 2124 Al alloy. At volume ratios greater than 5%, the number of crack initiation cycles decreases and the propagation rate increases.

Based on the literature review that has been conducted, it is observed that the previous studies have rarely performed comprehensive analyses of fatigue crack growth in FGM reinforced with various particles under diverse conditions. In this study, using the XFEM, the influence of parameters such as shape, size, and volume fraction of reinforcing particles on the fatigue life of these materials, in the presence of an initial crack, has been investigated.

The rest of paper is structured as follows. Section 2 introduces the XFEM as the primary analytical tool and elaborates on its fundamental concepts. Section 3 delves into the phenomenon of material fatigue and crack propagation mechanisms. Section 4 focuses on FGMs, examining the gradual distribution of material properties within various structures. Section 5 presents the numerical modeling of the problem, including plate geometry and crack, and analyzes the simulation results. Finally, Section 6 summarizes the research findings and presents the final conclusions.

2. Extended finite element method

The XFEM is a flexible numerical method aimed at accurately representing discontinuous behaviors in engineering problems. XFEM can effectively manage complicated geometries with high accuracy by enhancing the shape functions near discontinuities and utilizing partition of unity. In this approach, the main equations are expanded with extra degrees of freedoms to account for the abrupt behavior. However, the traditional FEM encounters difficulties when dealing with significant disruptions such as crack growth. The high computational costs and decreased accuracy are the outcomes of utilizing polynomial approximations and requiring a detailed mesh that mirrors the complicated crack shape. Moreover, the ongoing updating of the mesh while cracks are spreading makes the analysis procedure lengthy and complicated. Therefore, XFEM has become a viable option for studying problems with significant discontinuities and is widely used in different branches of engineering, such as structural mechanics, fluid mechanics, and thermal problems.

The basic principles of XFEM originate from Melenk and Babuška's work [25] on the Partition of Unity Finite Element Method (PUFEM) in the late 20th century. Nevertheless, Belytschko and Black [26] were the first to take innovative actions in this area by implementing discontinuous enrichment functions in the FEM, allowing for crack propagation simulation without requiring mesh restructuring. Moës [27] expanded on this technique and introduced the term "Extended Finite Element Method". Later on, Dolbow, Sukumar, and Stolarska [28-30] furthered the development and expansion of XFEM applications in different solid mechanics fields. These researcher used a variety of enrichment methods to create effective approaches for simulating individual and multiple cracks, voids, and other discontinuities [31]. Additionally, methods based on XFEM have been developed to predict crack propagation and adjust crack shape. For instance, enriched shape functions are commonly employed to represent the discontinuity associated with the crack, while the level set method utilizes a level set function to implicitly define the crack path. Additionally, the phase field method offers a diffuse interface approach to model crack propagation. These methods have been successfully applied to a wide range of engineering problems and have been extensively validated against experimental data [30, 32]. Overall, XFEM is now a useful tool for analyzing engineering problems

with significant variations, allowing for accurate and efficient modeling without the need for frequent mesh modifications.

XFEM enhances the FEM displacement field to accommodate weak discontinuities caused by inclusions and strong discontinuities due to cracks. Eq. (1) represents the general formulation of XFEM [33].

$$u^h(x) = u^{FE}(x) + u^{enr}(x) = \sum_{i=1}^{n} N_i(x) u_i + \sum_{j=1}^{p} N_j(x) \varphi(x) q_j, \quad (1)$$

where $u^{FE}(x)$ is the displacement field for the FEM, $u^{enr}(x)$ is the enrichment displacement field for the XFEM, $N_i(x)$ and $N_i(x)$ are shape functions for nodes i and j, respectively, u_i is the displacement field for the FEM nodes, $\varphi(x)$ is the enrichment function (which is changed for different problems), q_j is the displacement field for the XFEM nodes, and n and p denote the number of nodes for the FEM and XFEM, respectively.

In the context of crack propagation problems, the XFEM partitions elements into three distinct regions based on their proximity to the crack: a standard continuous region, a region intersected by the crack, and a region encompassing the crack tip. This elemental classification enables the modification of Eq. (1) to yield Eq. (2).

$$u_{xfem}(x) = u^{FE}(x) + u^{H}(x) + u^{tip}(x), \quad (2)$$

where $u^{H}(x)$ is the approximate displacement field for the elements intersected by cracks, and $u^{tip}(x)$ is the approximate displacement field for the elements containing a crack tip. To accurately represent displacement fields, two enrichment functions, F(x) and H(x) (depicted in Fig. 1a), are introduced. F(x) addresses the stress singularity at the crack tip, while H(x) accounts for the displacement jump across crack surfaces within fully cut elements. The displacement field for both $F(x)$ and $H(x)$ is defined by Eq. (3).

$$u_{xfem}(x) = \sum_{i \in I} N_i(x) u_i + \sum_{j \in I_{step}} N_j(x) H(x) a_j + \sum_{k \in I_{tip}} N_k(x) F(x) b_k. \quad (3)$$

In this formulation, the sets I, I_{step}, and I_{tip} represent conventional continuous elements, elements enriched

by $H(x)$, and elements enriched by $F(x)$, respectively. The displacement fields of the elements enriched by $H(x)$ and $F(x)$ are denoted by a_j and b_k, respectively. $N_j(x)$ and $N_k(x)$ represent the shape functions associated with nodes j and k.

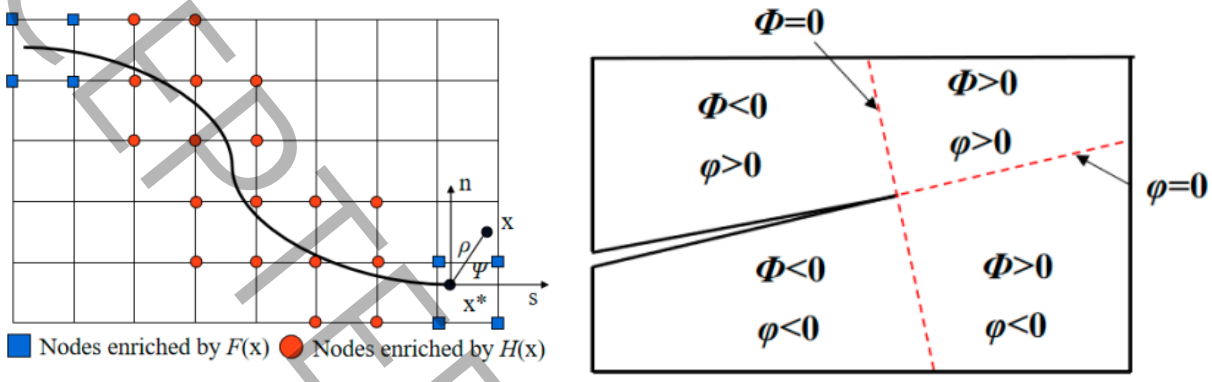

(a) (b)

Fig. 1. Principle figure of XFEM. (a) Classification of enrichment elements. (b) Level set Function of crack tip [14].

Equation (4) represents the formula of $H(x)$.

$$H(x)=\begin{cases}1 & \text{if } (x-x^*)\cdot n\geq 0\\ -1 & \text{other conditions}\end{cases} \tag{4}$$

where x denotes the integration point, x^* is the point that is closest to x on the crack surface, and n is the normal vector of x^*. Equation (5) is the formula of $F(x)$, which applies to isotropic material.

$$F(x)=\left[\sqrt{\rho}\sin\frac{\psi}{2}\sqrt{\rho}\cos\frac{\psi}{2}\sqrt{\rho}\sin\psi\sin\frac{\psi}{2}\sqrt{\rho}\sin\psi\cos\frac{\psi}{2}\right], \tag{5}$$

where ρ and ψ are the local polar coordinates of point x with respect to the crack tip. One main difference between FEM and XFEM is that XFEM can avoid the necessity of remeshing. This is accomplished by utilizing a level set function. The enrichment functions employed within the XFEM are explicitly defined in terms of this level set function. Consequently, updates to the level set function during crack growth automatically adjust the enrichment, as demonstrated in [30]. The crack front is represented using two level set functions. The first, denoted by $\varphi(x,t)$, defines the crack surface, where x corresponds to the mesh

nodes and t represents time. A point is considered above the crack surface when the value of $\phi(x,t)$ is positive, and conversely, it is below the surface when the value is negative (see Fig. 1b). The orthogonal surface is described by the level set function $\phi(x,t)$ (Fig. 1b). Equations (6) and (7) give the explicit formulas for both level set functions.

$$\varphi(x,t) = (x - x_{tip}) \cdot t, \tag{6}$$

$$\phi(x,t) = \pm \| x - x_i \|, \tag{7}$$

where x_{tip} is the coordinate of the crack tip, and x_i is the point on the crack path.

3. Fatigue crack growth

In this research, Paris' law is utilized to predict the rate of crack growth. The Umixmodefatigue subroutine is employed to calculate the maximum and minimum stress intensity factors caused by cyclic loading. The maximum principal stress theory is used to identify the crack propagation path at specific locations along the crack tip. This theory suggests that the crack expands at a right angle to the direction of the highest principal stress. As a result, the same Mode I stress intensity factor and crack growth angle are determined by utilizing Eq. (8) and Eq. (9).

$$K_{Ieq} = K_I \cos^3\left(\frac{\theta_c}{2}\right) - 3K_{II} \cos^2\left(\frac{\theta_c}{2}\right) \sin\left(\frac{\theta_c}{2}\right), \tag{8}$$

$$\theta_c = 2\tan^{-1}\left(\frac{K_I - \sqrt{K_I^{\,2} - 8K_{II}^2}}{4K_I}\right), \tag{9}$$

where, K_I and K_{II} are the Mode I and Mode II stress intensity factors, respectively. From Eq. (8) the equivalent SIF can be found as:

$$\Delta K_{Ieq} = \Delta K_I \cos^3\left(\frac{\theta_c}{2}\right) - 3\Delta K_{II} \cos^2\left(\frac{\theta_c}{2}\right) \sin\left(\frac{\theta_c}{2}\right). \tag{10}$$

For stable crack propagation, the generalized Paris' law is given as:

$$\frac{da}{dN} = C(x)(\Delta K)^{m(x)}, \tag{11}$$

where, $C(x)$ and $m(x)$ are the functions of the location. In numerical computations, a value is assumed for crack growth increment Δa and Eq. (11) is used to determine the corresponding cycles count, ΔN. When multiple crack tips exist, the main crack tip is identified and the value of ΔN is calculated from this. The growth of other crack tips is then assessed using the same ΔN value. The simulation stops when the maximum K_{Ieq} for any crack tip surpasses the local fracture toughness, K_{Ic}. This marks the end of the FGM's fatigue life.

4. Material properties of FGM

This research examines an FGM plate, shown in Fig. 2, with properties that change gradually from aluminum to alumina. By incorporating different quantities of alumina in the x-direction, a gradient in material characteristics is produced in this plate made of strengthened aluminum alloy. The USDFLD subroutine in ABAQUS finite element analysis software is utilized to accurately determine the characteristics of the FGM and incorporate the continuous variation of properties. The USDFLD subroutine is a useful tool that allows the user to establish varied connections between material characteristics and field variables like coordinates. It is noted that, a custom subroutine is used to specify the gradual change in material characteristics from aluminum to alumina. By using this subroutine, the material properties could change based on spatial coordinates, creating a smooth shift from metallic aluminum at x=0 to ceramic alumina at x=L. In all analyses, a starting crack is assumed at the middle of the FGM plate, going through its entire thickness. Table 1 lists the mechanical characteristics of the silicon nitride particle-reinforced FGM.

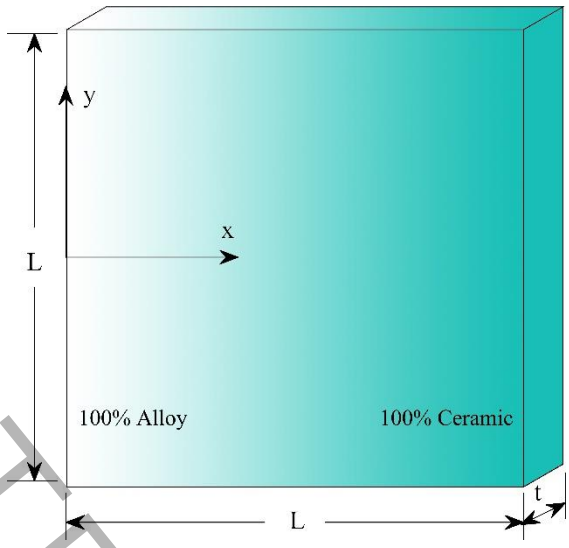

Fig. 2. Geometry of the FGM plate along with its dimensions.

Table 1. Quantified parameters in two segments [34-36]

Materials Properties	Aluminum alloy	Alumina	Silicon nitride
E(GPa)	70	300	270
υ	0.33	0.21	0.27
Fracture toughness K_{Ic}	29	3.5	5.7
Paris law parameter C	10^{-10}	2.8×10^{-12}	1.01×10^{-21}
Paris law parameter m	3	10	12-18

The variation of the elastic modulus for FGM is assumed as [34]:

$$E(x)=E_{alloy}e^{\alpha x},\alpha=\frac{1}{L}\ln\left(\frac{E_{ceramic}}{E_{alloy}}\right). \tag{12}$$

Given the gradient composition of the FGM, the local elastic modulus is approximated using a rule of mixtures based on the local alumina volume fraction. The varying volume fractions of ceramic and aluminum alloy are consequently determined as:

$$V_{Ceramic}^{FGM}(x)=\frac{E(x)-E_{alloy}}{E_{ceramic}-E_{alloy}}=\frac{E_{alloy}e^{\alpha x}-E_{alloy}}{E_{ceramic}-E_{alloy}}, \tag{13}$$

$$V_{alloy}^{FGM}(x)=1-V_{Ceramic}^{FGM}(x). \tag{14}$$

The Poisson's ratio of the FGM is computed as follows:

$$\upsilon(x)=\frac{\upsilon_{alloy}V_{alloy}^{FGM}(x)E_{ceramic}+\upsilon_{ceramic}V_{Ceramic}^{FGM}(x)E_{alloy}}{V_{alloy}^{FGM}(x)E_{ceramic}+V_{Ceramic}^{FGM}(x)E_{alloy}}. \tag{15}$$

The fracture toughness of the FGM can be correlated to the volume fraction of the ceramic component, as described by the following equation.

$$K_{Ic}(x)=\frac{K_{Ic}^{\ alloy}+K_{Ic}^{\ ceramic}}{2}+\frac{K_{Ic}^{\ alloy}-K_{Ic}^{\ ceramic}}{2}\times\left(\sqrt{1-V_{Ceramic}^{FGM}(x)}-\sqrt{V_{Ceramic}^{FGM}(x)}\right). \tag{16}$$

Paris law parameters exhibit an exponential correlation with elastic modulus, thus their variation is assumed to follow an exponential trend.

$$C(x)=C_{alloy}e^{\vartheta x},\vartheta=\frac{1}{L}\ln\left(\frac{C_{ceramic}}{C_{alloy}}\right), \tag{17}$$

$$m(x)=C_{alloy}e^{\zeta x},\zeta=\frac{1}{L}\ln\left(\frac{C_{ceramic}}{C_{alloy}}\right). \tag{18}$$

5. Problem description, results and discussions

This study considers a square FGM plate with dimensions of 30 μm × 30 μm. The plate exhibits a compositional gradient, transitioning from 100% aluminum alloy on the left side to 100% alumina ceramic on the right side, reinforced with silicon nitride particles. A fully clamped boundary condition is applied to the bottom edge of the plate, and plane strain conditions are assumed throughout the simulation. The material properties are graded along the x-direction, varying from 0 μm to 30 μm. The silicon nitride reinforcement particles are distributed randomly within the FGM plate using a numerical algorithm. This algorithm ensures a uniform distribution of particles, preventing overlapping. The center positions of the particles are determined using random numbers within the plate's dimensions. To avoid overlapping, a

minimum distance between particle centers is enforced. The reinforcement particles are modeled as squares, triangles, and circles with fixed side length, triangular edge length and radius. The number of reinforcement particles is determined based on the desired volume fraction. An initial crack with a length of 6 μm is introduced at the left edge of the FGM plate. XFEM is employed for crack modeling, eliminating the need for remeshing during crack growth. XFEM utilizes enrichment functions to model discontinuities such as cracks. Specific enrichment functions are used to accurately represent the singular stress field around the crack tip. These enrichment functions are automatically updated as the crack propagates. The finite element analysis is performed using Abaqus software. The plate is discretized using four-node bilinear plane strain elements (CPE4R). A cyclic Mode I tensile load, ranging from σ_{min} = 0 MPa to σ_{max} = 70 MPa, is applied to the upper edge of the plate. The cyclic loading is defined using a tabular amplitude in Abaqus, with the following points: (0, 0), (0.5, 1), and (1, 0). The direct cycles solver in Abaqus is used to analyze the fatigue behavior of the FGM plate under cyclic loading. Two predefined fields are defined to assign distinct fatigue properties to the reinforcing particles and the FGM matrix. The first field is reinforcement particle field. This field identifies the regions occupied by the silicon nitride particles. Fatigue properties specific to the particle material are assigned to this field. The second field is FGM matrix field. This field defines the remaining volume of the FGM plate, representing the graded aluminum-alumina matrix. Fatigue properties corresponding to the local material composition within the gradient are assigned to this field. By utilizing these predefined fields, the simulation accurately captures the heterogeneous fatigue behavior of the FGM plate, considering the distinct properties of both the reinforcing particles and the graded matrix.

5-1- Validation

To validate the finite element model for fatigue crack growth in FGMs using the XFEM, a simulation is conducted and the results are compared with those reported by Bhattacharya et al. [34]. The present model simulates the fatigue life of an FGM plate with an initial crack located at the mid-plane. To analyze the fatigue strength of the FGM plate under cyclic loading, the fatigue life of the FGM plate is compared with that of an aluminum plate with various crack lengths and locations. As shown in Fig. 3, the fatigue life-

crack growth rate curve of the simulated model exhibits good agreement with the results reported in the reference paper.

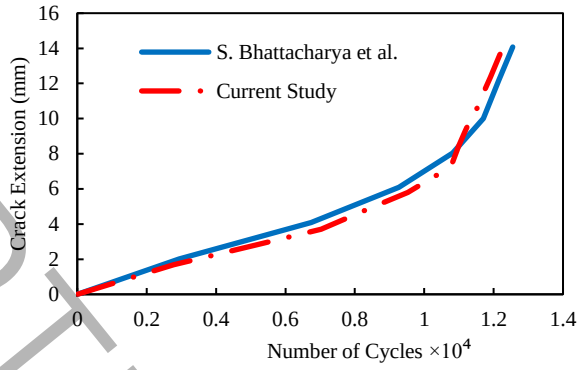

Fig. 3. Fatigue life vs. crack growth rate comparison for a simulated FGM plate and the model proposed by Bhattacharya et al. [34].

5-2- Analysis of unreinforced FGM plates

Initially, in order to determine the increase in fatigue life due to the addition of reinforcing particles, the fatigue life of the plate without reinforcing particles must be calculated. Figure 4 depicts an FGM plate with an edge crack located on the alloy-rich side, along with its corresponding boundary conditions. The FGM plate is fully clamped at the bottom edge and subjected to cyclic loading on the top surface. The mean fatigue life plot is presented in Fig. 5. Simulation results indicate that the equivalent FGM plate can withstand 353,010 cycles before failure. Figure 6 illustrates the crack propagation path for the FGM plate.

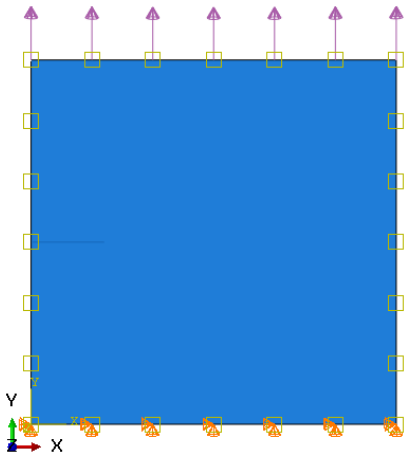

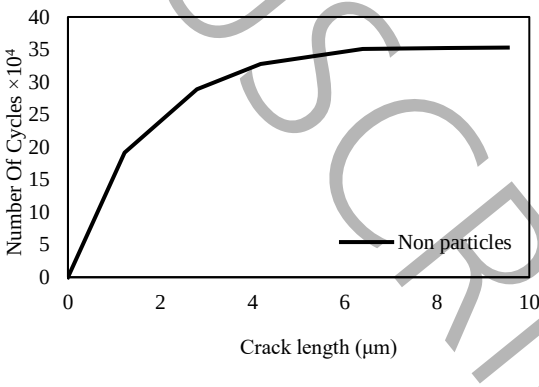

Fig. 4. Model geometry and dimensions.

Fig. 5. Fatigue crack growth rate versus cycles to failure.

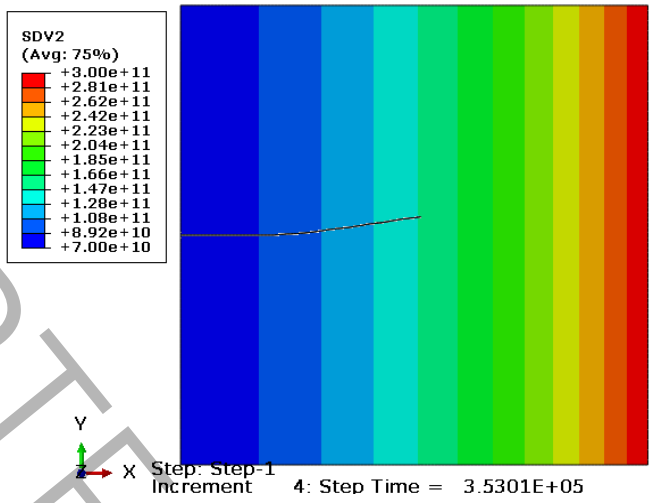

Fig. 6 Crack growth in an FGM plate.

5-3- analysis of square particles reinforced FGM plates

The initial phase of model creation involves a random distribution of reinforcement particles within the plate using a numerical algorithm, subject to the constraints of the plate and particle dimensions. This arrangement guarantees that the particles remain completely enclosed by the plate and do not cross initial crack path. Reinforcements are randomly distributed in the form of silicon nitride particles. The convergence of the mesh for the FGM plate reinforced with 10% of 2.66 μm square particles is then examined. As shown in Fig. 7, the number of fatigue life cycles initially increases significantly with the increase in element count. However, after reaching an element count of 12,200, the increase in the number of cycles becomes minimal. This indicates that up to 12,200 elements, the accuracy of the calculations improves considerably, leading to more precise results. Beyond this point, the enhancement in computational accuracy is negligible, resulting in only a slight increase in the number of cycles. Therefore, an element number of 12,200 is selected as the optimal size, as it provides a good balance between computational accuracy and processing time. To further validate the results, calculations were also performed with an element count of 14,100. As illustrated in Fig. 7, the number of cycles at this mesh size does not differ significantly from that at the 12,200 elements count. This confirms that the element number

of 12,200 is optimal, and the results obtained are acceptably accurate. Hence, all further calculations are conducted with this mesh number and size. To study how the size and volume fraction of square reinforcement particles affect crack growth and fatigue life of the FGM plate, 9 samples are analyzed. For this purpose, volume fractions of 10%, 20%, and 30% and the sizes of 0.89 μm, 1.77 μm, and 2.66 μm of silicon nitride particles are considered. Figure 8 schematically illustrates the distribution of silicon nitride particles and the corresponding crack growth path within the plate for particles of size 1.77 μm and various volume fractions.

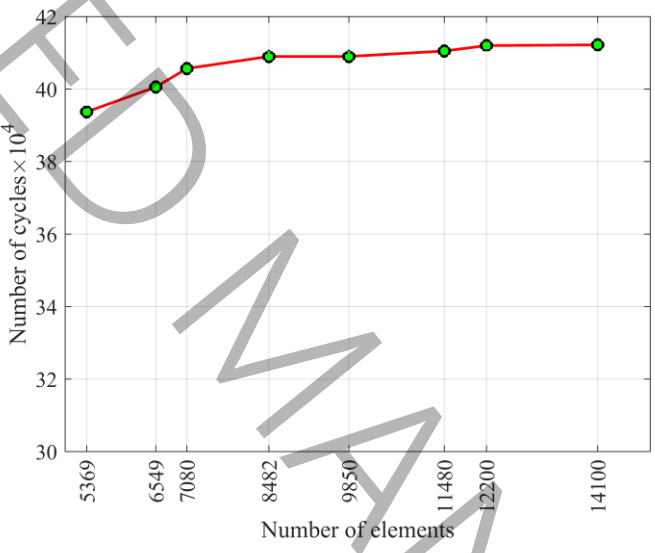

Fig. 7. Convergence study for an edge crack problem.

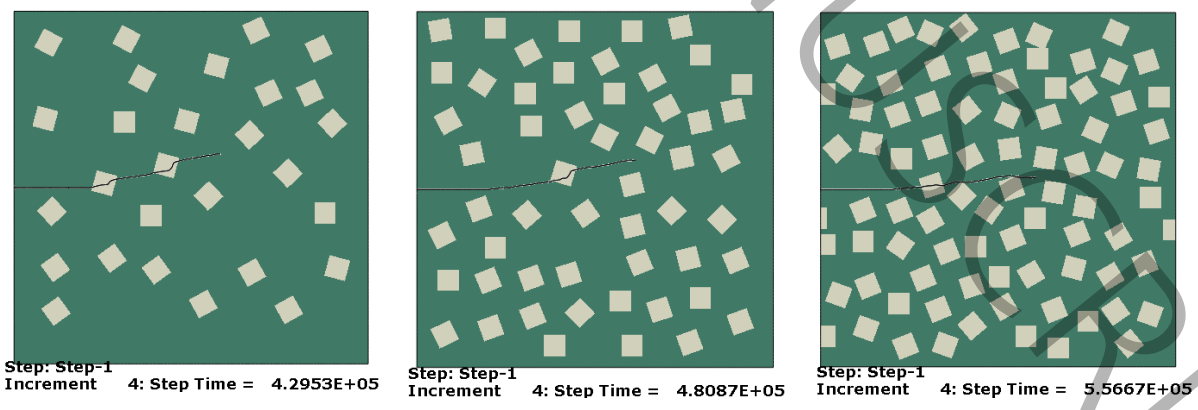

(a) (b) (c)

Fig. 8. Distribution of silicon nitride particles and fatigue crack growth path in an FGM plate containing 1.77 μm side

length particles with varying volume fractions a) 10%; b) 20%; c) 30%.

Figures 9,10 and 11 depict the fatigue life of the FGM plate reinforced with silicon nitride particles of varying volume fractions and sizes. These results indicate that the size of the reinforcement particles has a substantial influence on the crack growth behavior and fatigue life. Significantly, 0.89 μm particles show the biggest improvement in fatigue life when compared to 2.66 μm particles, resulting in enhancements of 11.34%, 7.79%, and 10.86% at 10%, 20%, and 30% volume fractions, respectively. Fatigue life improvement remains relatively constant when particle size exceeds 0.89 μm. The findings shown in Figs. 12 to 14 clearly indicate the crucial influence of the volume fraction of reinforcement particles on reducing crack propagation. By increasing the percentage of silicon nitride particles in an FGM plate and keeping the particle size constant, the fatigue life was significantly prolonged. For example, at a 30% higher volume fraction, there was a boost of 70.47%, 57.69%, and 53.76% in fatigue life for particle sizes of 0.89, 1.77, and 2.66 μm, respectively, in comparison to the plate without reinforcement.

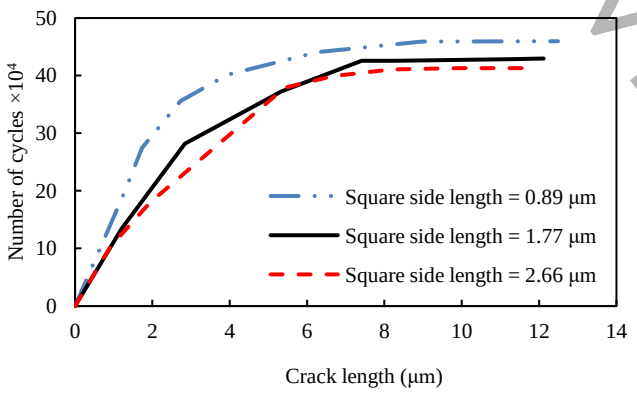

Fig. 9. Effect of square particle size on fatigue life of FGM plates with 10% silicon nitride reinforcement.

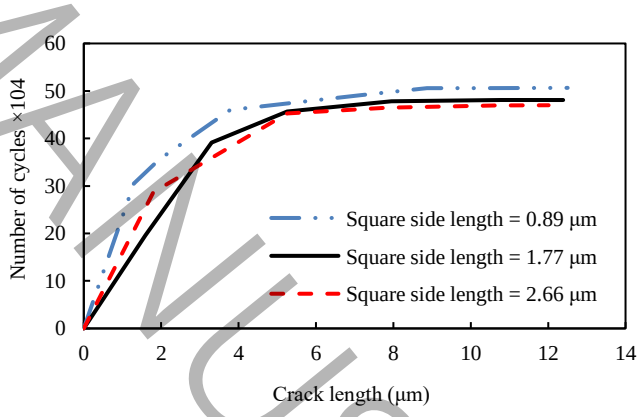

Fig. 10. Effect of square particle size on fatigue life of FGM plates with 20% silicon nitride reinforcement.

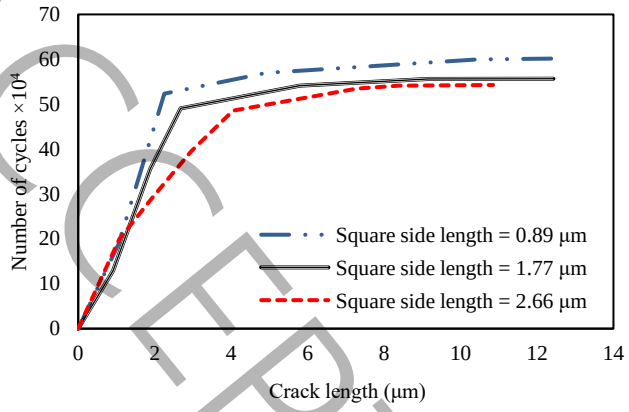

Fig. 11. Effect of square particle size on fatigue life of FGM plates with 30% silicon nitride reinforcement.

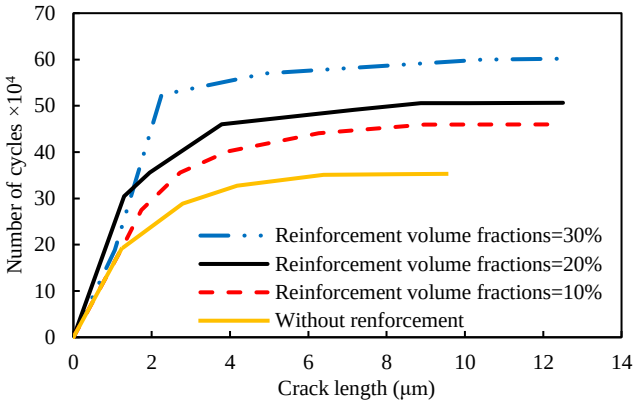

Fig. 12. Effect of square silicon nitride particle volume fraction on fatigue life for a constant particle size of 0.89 μm.

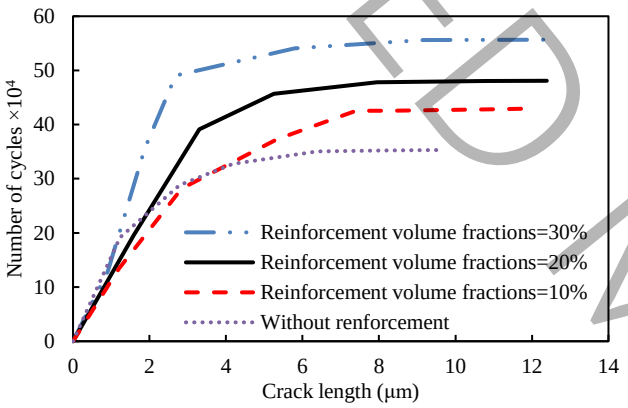

Fig. 13. effect of square silicon nitride particle volume fraction on fatigue life for a constant particle size of 1.77 μm.

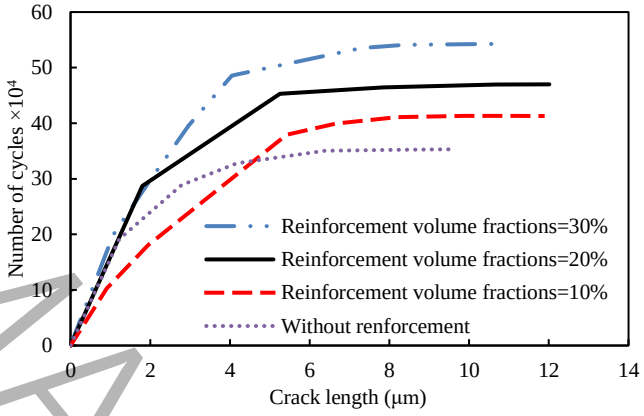

Fig. 14. Effect of square silicon nitride particle volume fraction on fatigue life for a constant particle size of 2.66 μm.

5-4- Analysis of circular particles reinforced FGM plates

In this section, similar to the square particles, a numerical algorithm is utilized to simulate the random arrangement of circular silicon nitride reinforcement particles in the plate's matrix. This algorithm is designed to randomly disperse the particles on the plate with no overlapping geometric shapes. The circular-shaped reinforcement particles, assuming equal surface areas with the square particles, have been simulated with radius of 0.5, 1, and 1.5 μm, and volume fractions of 10%, 20%, and 30%. Figure 15 schematically illustrates the distribution of 0.5 μm silicon nitride particles and the corresponding crack propagation path within the plate for various volume fractions.

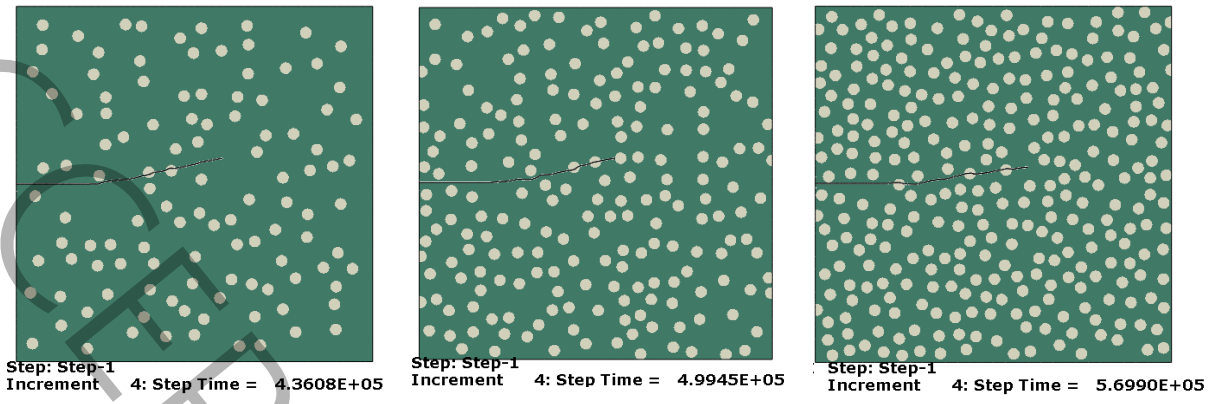

(a) (b) (c)

Fig. 15. Distribution of silicon nitride particles and fatigue crack growth path in an FGM plate containing 0.5 μm particles with varying volume fractions a) 10%; b) 20%; c) 30%.

Fatigue life diagrams of FGM plates in the presence of silicon nitride reinforcement particles with three different volume fractions and sizes are presented in the Figs. 15 to 20. Based on Figs. 15 to 17, it is observed that the addition of circular silicon nitride particles as reinforcements in FGM plates significantly enhances the fatigue resistance of these plates. The reason for this strengthening effect is believed to be the particles ensuring a more even distribution of stress in the FGM matrix, thus avoiding stress buildup at key points and the start of fatigue cracks. Numerical studies indicate that reducing the size of silicon nitride particles improves their ability to reinforce FGM plates. Particles measuring 0.5 μm in radius resulted in fatigue life enhancements of 6.90%, 8.76%, and 6.15% at volume fractions of 10%, 20%, and 30%, respectively, when compared to particles of 1.5 μm in radius. The boost is mainly due to the larger contact area between the particles and the FGM matrix as the particle size decreases. Moreover, Figs. 18 to 20 show a direct relationship between the fatigue life of the FGM plate and the volume fraction of silicon nitride particles. In other words, an increased amount of reinforcing particles in the matrix improves the plate's ability to resist crack propagation, thus prolonging its fatigue life. As an example, plates containing particles amounting to 30% of their volume show increases in fatigue life by 61.14%, 56.73%, and 52.08%, when compared to plates without reinforcement, using particles with radius of 0.5, 1, and 1.5 μm, respectively. Based on the findings of this investigation, the mechanical characteristics of FGM plates are considerably

enhanced when circular silicon nitride particles are used as reinforcement, with a particular improvement in fatigue resistance. There is a particular improvement in fatigue resistance. The results imply that silicon nitride-reinforced FGM materials may find broader uses across several industrial domains.

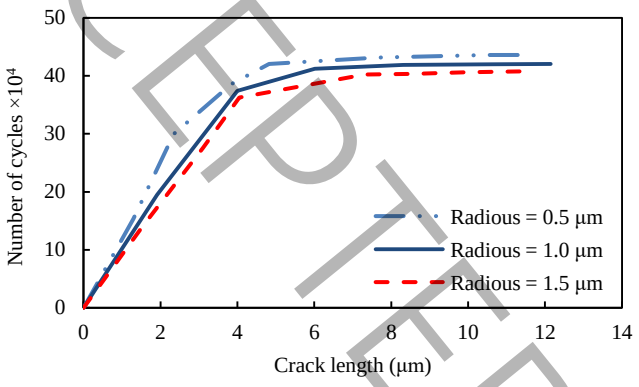

Fig. 15. Effect of circular particles size on fatigue life of FGM plates with 10% silicon nitride reinforcement.

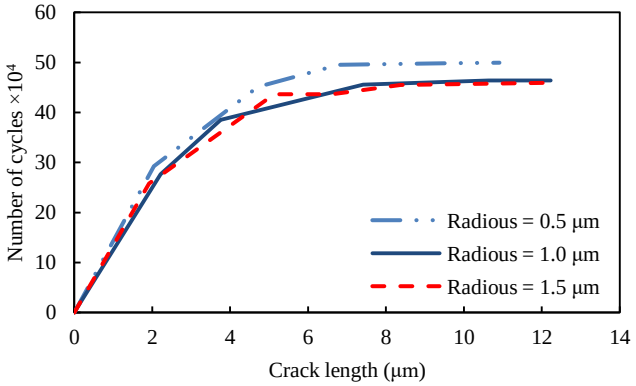

Fig. 16. Effect of circular particles size on fatigue life of FGM plates with 20% silicon nitride reinforcement.

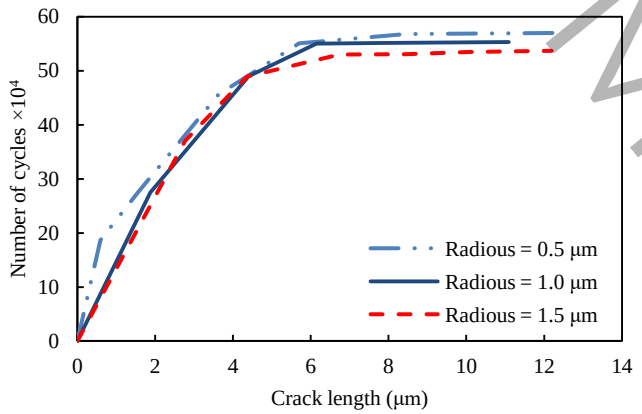

Fig. 17. Effect of circular particles size on fatigue life of FGM Plates with 30% silicon nitride reinforcement.

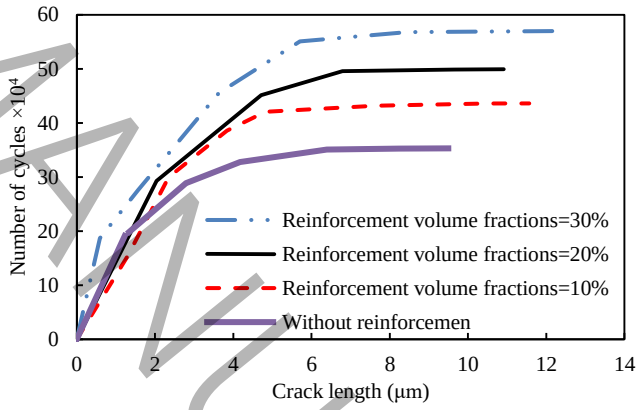

Fig. 18. Effect of circular particles volume fraction on fatigue life for a constant particle size of 0.5 μm.

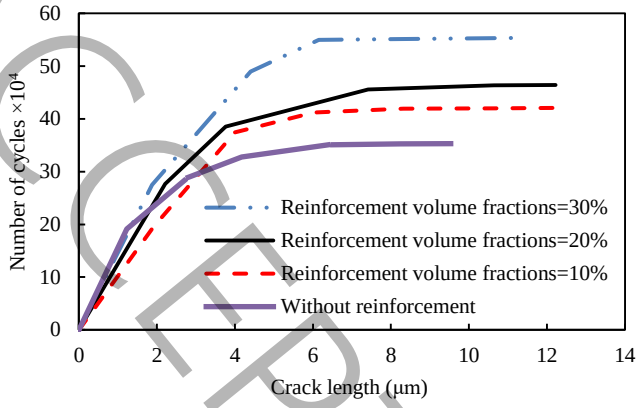

Fig. 19. Effect of circular particles volume fraction on fatigue life for a constant particle size of 1 μm

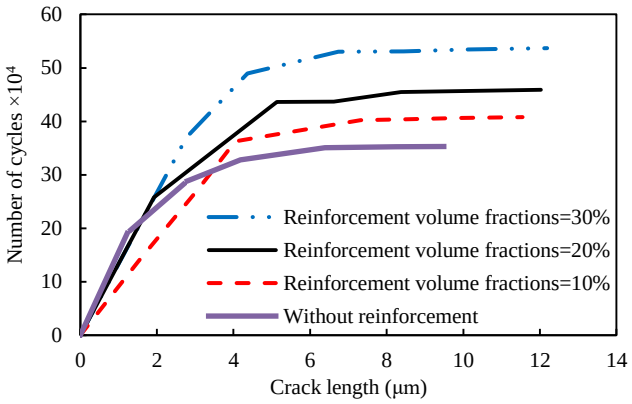

Fig. 20. Effect of circular particles volume fraction on fatigue life for a constant particle size of 1.5 μm.

5-5- Analysis of triangle particles reinforced FGM plates

In this section, an initial crack of 6 μm is introduced at the left edge of a small square plate (30 μm × 30 μm). Subsequently, ceramic reinforcement particles (silicon nitride) are randomly distributed within the plate using numerical methods. These particles are triangular in shape and considered at three volume fractions of 10%, 20%, and 30%. Assuming the area of triangular particles is equal to that of square and circular particles, the edge length of these triangular reinforcement particles was considered to be 1, 2, and 3 μm. A critical aspect of this modeling was ensuring that the particles were entirely contained within the plate and did not overlap. The distribution of silicon nitride particles with the size of 0.5 micrometers and the associated crack propagation path within the plate for different volume fractions are schematically shown in Fig. 21.

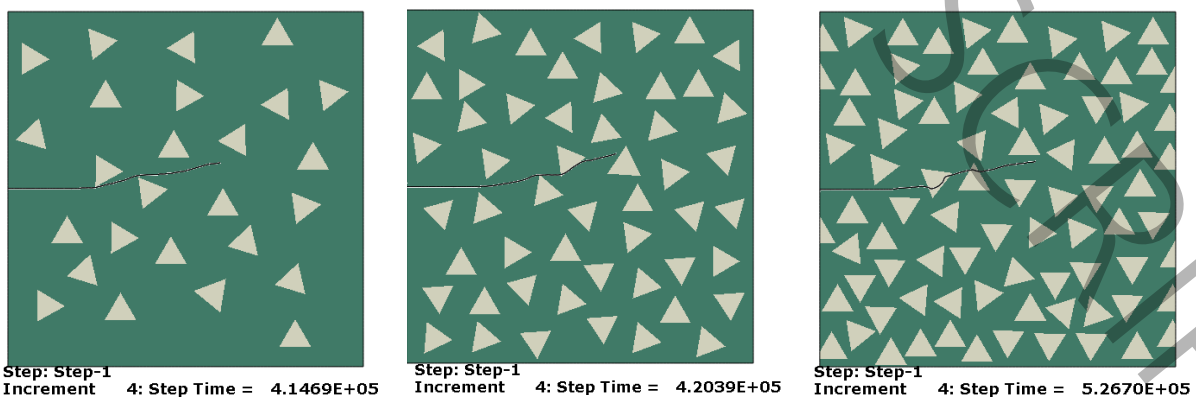

(a) (b) (c)

Fig. 21. Distribution of triangular silicon nitride particles and fatigue crack growth path in an FGM plate containing 2.66 μm particles with varying volume fractions a) 10%; b) 20%; c) 30%.

Results from the simulations, shown in Figs. 22 to 24, clearly show that adding reinforcing triangular particles to FGM boosts fatigue resistance. This improvement becomes significantly more noticeable as the particle size decreases. In particular, particles with 1.35 μm radius show the greatest enhancements in fatigue life compared to 4.04 μm particles at 10%, 20%, and 30% volume fractions, leading to increases of 4.07%, 18.26%, and 6.72%, respectively. Figures 25-27 further corroborate the direct correlation between increasing the volume fraction of triangular particles and enhanced fatigue life of the FGM. In essence, a higher concentration of reinforcing particles results in greater resistance to fatigue crack propagation in the FGM. Significantly, the plate containing 30% particles shows the greatest enhancements in fatigue life compared to the plate without particles, with boosts of 53.70%, 49.20%, and 47.67% for particle sizes of 1.35, 2.66, and 4 μm, respectively.

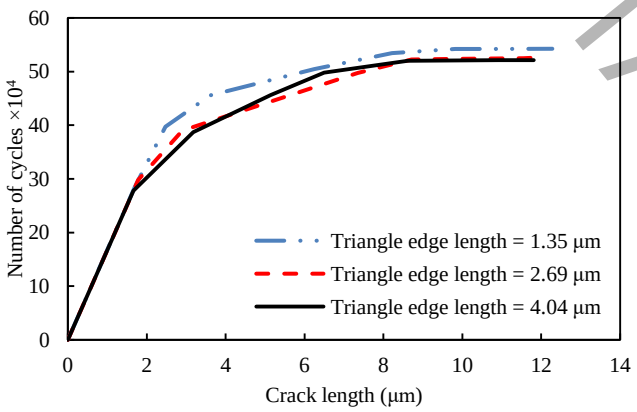

Fig. 22. Effect of triangular particle size on fatigue life of FGM plates with 10% silicon nitride reinforcement.

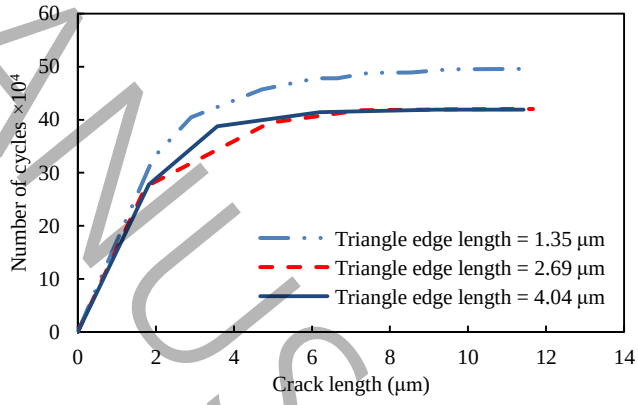

Fig. 23. Effect of triangular particle size on fatigue life of FGM plates with 20% silicon nitride reinforcement.

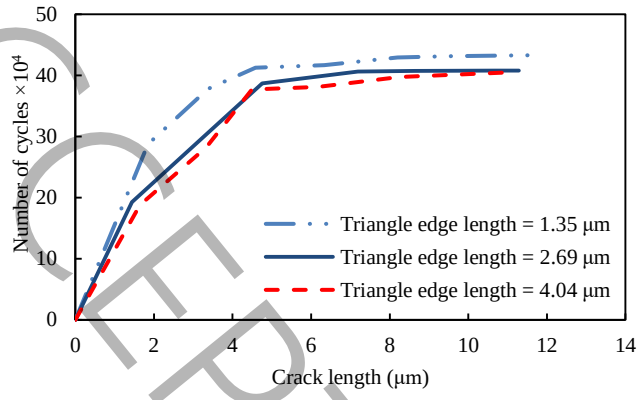

Fig. 24. Effect of triangular particle size on fatigue life of FGM plates with 30% silicon nitride reinforcement.

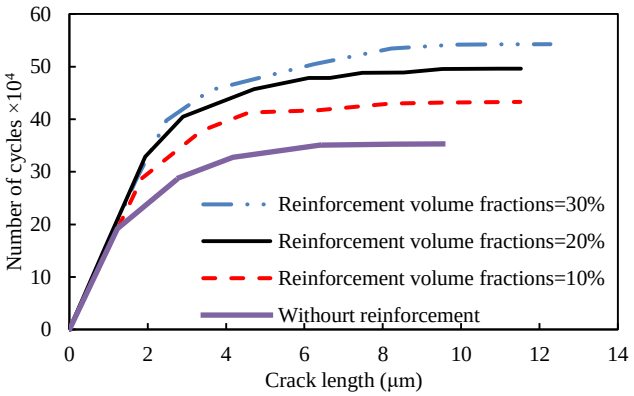

Fig. 25. Effect of triangular particle volume fraction on fatigue life for a constant particle size of 1.35 μm.

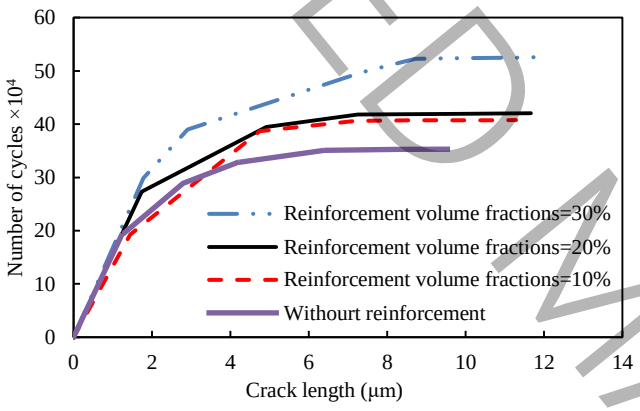

Fig. 26. Effect of triangular particle volume fraction on fatigue life for a constant particle size of 2.66 μm.

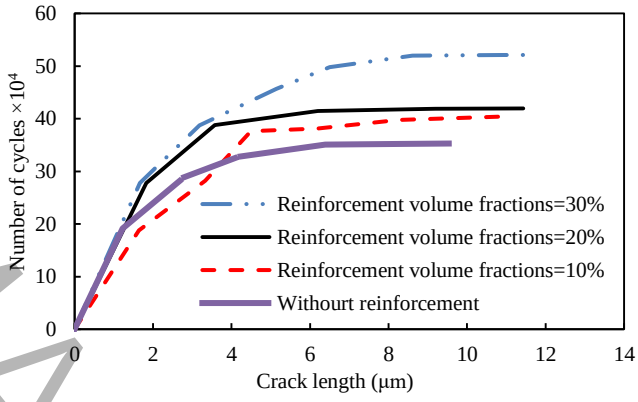

Fig. 27. Effect of triangular particle volume fraction on fatigue life for a constant particle size of 4.04 μm.

5-5- Effect of reinforcer geometry on the fatigue life of FGM plates

The geometry of silicon nitride reinforcement particles has been identified as a critical parameter in governing the fatigue behavior of FGM plates. Analysis of simulation data (Figs. 28 and 29) reveals that rectangular particles, owing to their more effective stress distribution around crack tips, result in a significant enhancement in fatigue life. Rectangular particles covering 30% of the plate volume showed notable improvements in fatigue life. More precisely, these particles measuring 0.89 μm resulted in a 70.47% boost in fatigue life. Although circular and triangular particles showed enhancements of 61.44% and 53.70%, respectively, rectangular particles displayed the most significant impact, as shown in Fig. 28.

Comparable studies were carried out on strengthening particles measuring 2.66 μm, with the findings displayed in Fig. 29. In this case, rectangular particles, taking up 30% of the plate volume, still showed better performance, with a 30.24% boost in fatigue life. The increase was significantly greater than that seen in circular and triangular particles, which showed enhancements of 23.53% and 22.62%, respectively. Examination of different levels with different particle sizes showed comparable results. Rectangular particles show better performance in the FGM because they distribute stress more evenly compared to circular and triangular particles. Rectangular particles can better disperse loads across the plate, resulting in higher strength and stiffness.

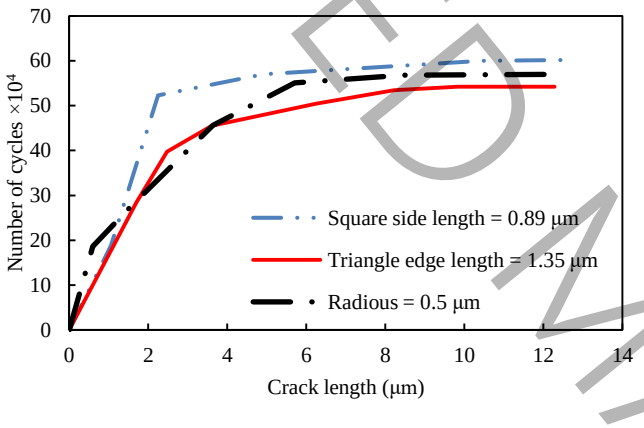

Fig. 28. Effect of particles shape on FGM fatigue life at 30% volume fraction.

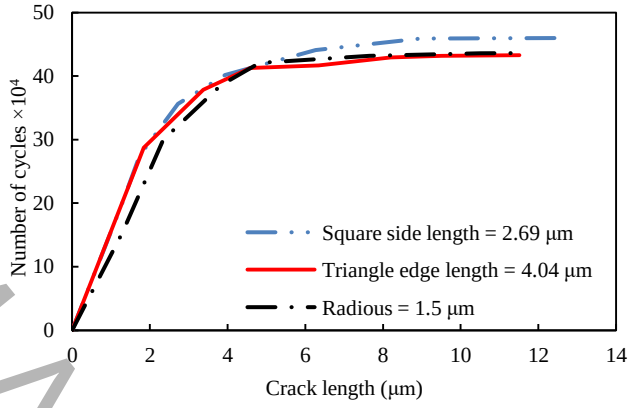

Fig. 29. Comparative study of various particle shapes in FGM fatigue life at 30% volume fraction.

5-6- Fatigue life of reinforced FGM plates under mixed-mode loading

As can be seen in Fig. 30, the application of cyclic shear loading significantly influences the fatigue behavior of the material. Compared to the results under purely tensile loading (Fig. 29), mixed-mode loading leads to a notable reduction in the number of cycles endured until failure. This decrease in fatigue life can be attributed to the alteration in failure mechanisms. Shear loading induces mixed-mode fracture (comprising a combination of tensile and shear fracture) instead of purely tensile fracture, consequently accelerating crack growth and diminishing fatigue life. Specifically, a comparison of the results reveals that shear loading results in an approximate 60% reduction in fatigue life, demonstrating the substantial impact

of shear loading on the fracture behavior of the material. For instance, square, circular, and triangular particles with sizes of 2.69 µm, 1.5 µm, and 4.04 µm, respectively, and a weight percentage of 30%, exhibited fatigue lives of 469,880, 459,191, and 419,430 cycles under tensile loading, while under shear loading, these values decreased to 204,670, 185,860, and 179,690 cycles, respectively. Nevertheless, similar to the previous results, square particles still demonstrated the most significant effect on the fatigue life of the plate, and triangular particles the least.

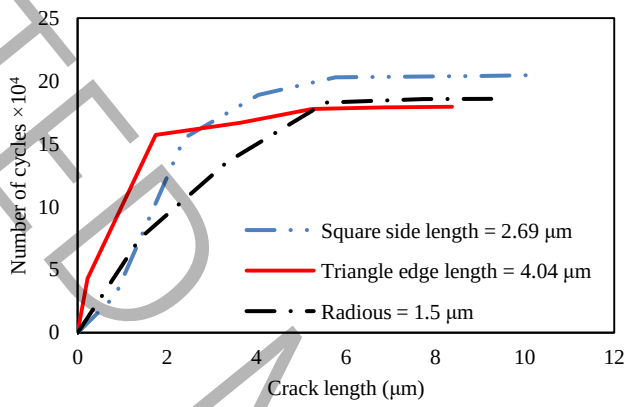

Fig. 30. Effect of particles shape on FGM fatigue life at 30% volume fraction under mixed-mode loading conditions.

5-7- Effect of particle size on fatigue life of FGM plates

To investigate the effects of size and to determine the lower limit of particle sizes, the square particles were reduced in three additional levels, and the fatigue life of the FGM plate was calculated. Fig. 31 shows the distribution of particles and the associated crack propagation path within the plate for different particle sizes. As demonstrated in the Fig. 32, reducing the size of square-shaped reinforcement particles at a 20% volume fraction continues to enhance fatigue life. These findings suggest that the trend of improved fatigue life persists with decreasing particle size. However, two primary challenges arise with the reduction of particle size. First, decreasing particle size directly results in an increased number of particles within a fixed matrix volume. This surge in particle count can lead to particle agglomeration and non-uniform particle distribution within the matrix, ultimately compromising the material's mechanical properties. Additionally, as particle size diminishes and particle count increases, the inter-particle spacing decreases, resulting in

meshing difficulties during numerical analyses. In other words, generating an appropriate and precise mesh around very small and closely spaced particles becomes challenging, potentially reducing the accuracy of the results. Considering these challenges, it can be concluded that there exists a lower limit for particle size, beyond which the reinforcing effect of the particles diminishes or other issues such as particle agglomeration and meshing difficulties arise. However, accurately determining this lower limit requires further investigation and more detailed analyses.

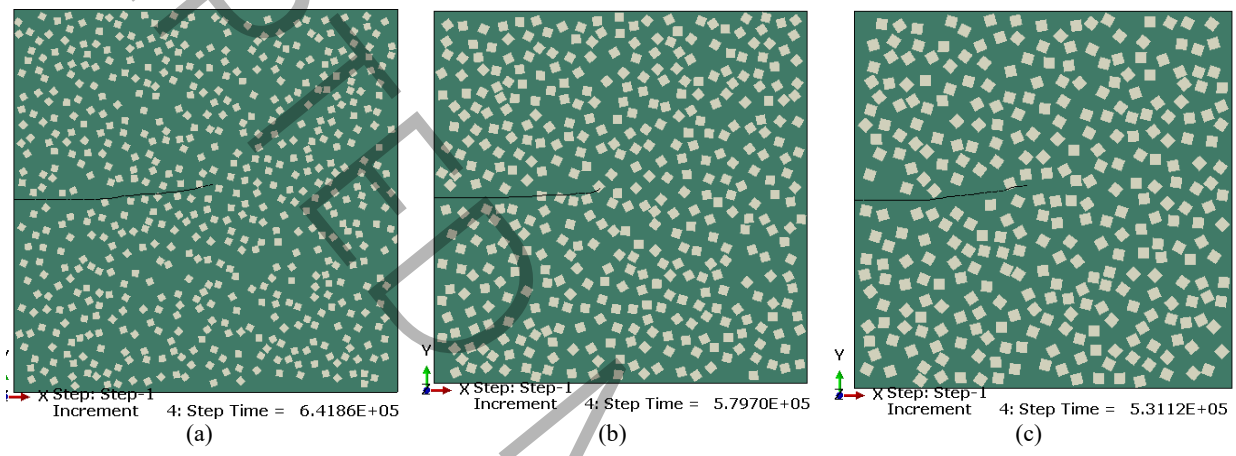

Fig. 31. Distribution of silicon nitride particles and fatigue crack growth path in an FGM plate containing 20% particles with varying square side length a) 0.62 μm; b) 0.71 μm; c) 0.80 μm.

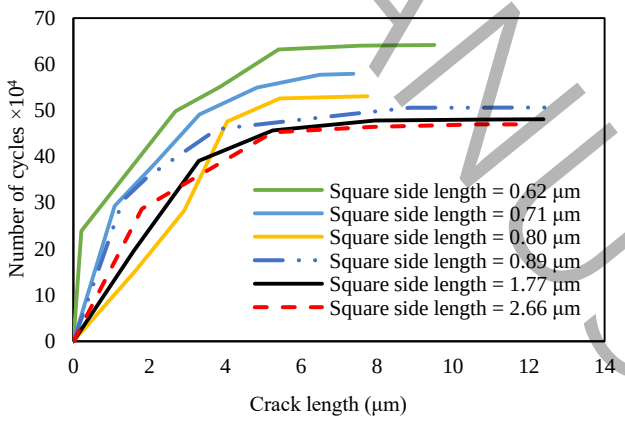

Fig. 32. Effect of square particle size on fatigue life of FGM plates with 20% reinforcement.

6. Conclusion

A comprehensive understanding of fatigue crack growth mechanisms is crucial for improving the service

life of structures made from FGMs. This research explored how the fatigue properties of FGMs reinforced with silicon nitride ceramic particles are influenced by the shape, size, and volume fraction of the reinforcing particles through numerical simulations. A random distribution of reinforcement particles within the plate was achieved using a numerical algorithm, constrained by the dimensions of the plate and particles. Three different shapes (square, triangular, and circular) and volume fractions of 10%, 20%, and 30% were examined with varying particle sizes, resulting in a total of 27 different cases. The loading was performed under cyclic tensile conditions. The convergence of the present results was assessed and the converged findings were compared with those available in the literature for simpler problem. From the detailed numerical study conducted, the following conclusions were drawn:

- Fatigue life increases with a decrease in particle size up to a certain point, beyond which it decreases again.
- As the size of the particles increases and reaches a specific threshold, the fatigue life remains relatively constant.
- Increasing the volume fraction of reinforcement particles significantly improved the fatigue life of the material.
- Square particles performed better in terms of fatigue resistance because of their optimized stress distribution and limited crack propagation.
- The plate with 30% square particles exhibited substantial improvements in fatigue life compared to the unreinforced plate, showing increases of 70.47%, 57.69%, and 53.76% for particle sizes of 0.89, 1.77, and 2.66 μm, respectively.
- Similarly, plates containing circular particles at 30% of their volume showed increases in fatigue life of 61.14%, 56.73%, and 52.08% when using particles with radii of 0.5, 1, and 1.5 μm, respectively.
- For triangular particles at a 30% volume fraction, fatigue life improved by 53.70%, 49.20%, and 47.67% compared to the unreinforced plate for particle sizes of 1.35, 2.66, and 4 μm, respectively.

- Square, circular, and triangular particles with sizes of 2.69 µm, 1.5 µm, and 4.04 µm, respectively, and a weight percentage of 30%, exhibited fatigue lives of 469,880, 459,191, and 419,430 cycles under tensile loading, while under shear loading, these values decreased to 204,670, 185,860, and 179,690 cycles, respectively.

The findings of this study can be utilized for designing and manufacturing engineering components under cyclic loading conditions. The results demonstrate a complex interactive relationship between particle size, volume fraction, and shape, which significantly affects the material's fatigue life.

References:

[1] I.V. Singh, B. Mishra, S. Bhattacharya, XFEM simulation of cracks, holes and inclusions in functionally graded materials, International Journal of Mechanics and Materials in Design, 7 (2011) 199-218.

[2] S. Bhattacharya, I.V. Singh, B. Mishra, Fatigue-life estimation of functionally graded materials using XFEM, Engineering with computers, 29 (2013) 427-448.

[3] Z. Wang, F. Liu, W. Liang, L. Zhou, Study on tensile properties of nanoreinforced epoxy polymer: macroscopic experiments and nanoscale FEM simulation prediction, Advances in Materials Science and Engineering, 2013 (2013).

[4] S. Bhattacharya, K. Sharma, Fatigue crack growth simulations of FGM plate under cyclic thermal load by XFEM, Procedia Engineering, 86 (2014) 727-731.

[5] M. Zakeri, A. Jafari, Investigation of stress field parameters in a cracked stiffened plate under mixed mode I/II, Aerospace Knowledge and Technology Journal, 5(2) (2016) 93-107.

[6] D. Bartaula, Y. Li, S. Koduru, S. Adeeb, Simulation of fatigue crack growth using XFEM, in: Pressure Vessels and Piping Conference, American Society of Mechanical Engineers, 2020, pp. V003T003A046.

[7] S. Bhattacharya, I. Singh, B. Mishra, T. Bui, Fatigue crack growth simulations of interfacial cracks in bi-layered FGMs using XFEM, Computational Mechanics, 52 (2013) 799-814.

[8] I. Bharti, N. Gupta, K. Gupta, Novel applications of functionally graded nano, optoelectronic and thermoelectric materials, International Journal of Materials, Mechanics and Manufacturing, 1(3) (2013) 221-224.

[9] A. Mohammadi Anari, E. Selahi, Crack initiation and growth simulations of functionally graded dental implant subjected to cyclic axial loads, Fatigue & Fracture of Engineering Materials & Structures, 45(11) (2022) 3123-3136.

[10] A. Shedbale, I.V. Singh, B. Mishra, Nonlinear simulation of an embedded crack in the presence of holes and inclusions by XFEM, Procedia Engineering, 64 (2013) 642-651.

[11] A.P. Singh, A. Tailor, C.S. Tumrate, D. Mishra, Crack growth simulation in a functionally graded material plate with uniformly distributed pores using extended finite element method, Materials Today: Proceedings, 60 (2022) 602-607.

[12] M. Zaidi, K.K. Joshi, A. Shukla, B. Cherinet, A review of the various modelling schemes of unidirectional functionally graded material structures, in: AIP Conference Proceedings, AIP Publishing, 2021.

[13] D. Kaka, R.A. Fatah, P. Gharib, A. Mustafa, Mechanical Properties of Polyester Toughened with Nano-Silica, Iraqi Journal of Industrial Research, 8(3) (2021) 61-68.

[14] A. Ulukoy, M. Topcu, S. Tasgetiren, An Experimental Crack Propagation Analysis of Aluminum Matrix Functionally Graded Material, Advances in Functionally Graded Materials and Structures, (2016).

[15] F. Xu, S. Zhu, J. Zhao, M. Qi, F. Wang, S. Li, Z. Wang, Effect of stress ratio on fatigue crack propagation in a functionally graded metal matrix composite, Composites Science and Technology, 64(12) (2004) 1795-1803.

[16] M. Bhattacharyya, A.N. Kumar, S. Kapuria, Synthesis and characterization of Al/SiC and Ni/Al2O3 functionally graded materials, Materials Science and Engineering: A, 487(1-2) (2008) 524-535.

[17] F. Xu, S. Zhu, J. Zhao, M. Qi, F. Wang, S. Li, Z. Wang, Fatigue crack growth in SiC particulates reinforced Al matrix graded composite, Materials Science and Engineering: A, 360(1-2) (2003) 191-196.

[18] A.P. Agrawal, S.K. Srivastava, Investigations of fatigue crack growth rate behaviour and life prediction of Si3N4/TiB2 reinforced hybrid metal matrix composites, International Journal of Fatigue, 186 (2024) 108373.

[19] A. Lal, N.M. Kulkarni, S. Singh, A. Mahto, R. Kumar, Mixed mode stress intensity factor analysis on edge cracked FGM plate with different material distribution models by XFEM, Journal of Mechanical Science and Technology, (2024) 1-15.

[20] J. Lai, Y. Xia, Z. Huang, B. Liu, M. Mo, J. Yu, Fatigue life prediction method of carbon fiber-reinforced composites, e-Polymers, 24(1) (2024) 20230150.

[21] C. Chiu, V. Prabhakar, S. Tseng, F. Qayyum, S. Guk, C. Chao, U. Prahl, Integrating experimental and numerical analyses for microscale tensile behavior of ceramic particle reinforced TRIP steel composites: a study on local deformation and damage evolution, Composites Part A: Applied Science and Manufacturing, 186 (2024) 108384.

[22] E. Mosayyebi, T.N. Chakherlou, Numerical investigation of patch geometry effect on the fatigue life of aluminum panels containing cracks repaired with CFRP composite patch using XFEM and CZM approach, International Journal of Adhesion and Adhesives, 136 (2025) 103882.

[23] M. Bouchelarm, M. Chafi, A. Boulenouar, N. Benseddiq, Effect of the material gradation on the fracture trajectory in ceramic/metal functionally graded materials, Archives of Metallurgy and Materials, (2024) 955-963-955-963.

[24] A. Karci, V. Erturun, E. Çakir, Y. Çam, Fatigue crack growth rate and propagation mechanisms of SiC particle reinforced Al alloy matrix composites, Aircraft Engineering and Aerospace Technology, 96(2) (2024) 185-192.

[25] J.M. Melenk, I. Babuška, The partition of unity finite element method: basic theory and applications, Computer methods in applied mechanics and engineering, 139(1-4) (1996) 289-314.

[26] T. Belytschko, T. Black, Elastic crack growth in finite elements with minimal remeshing, International journal for numerical methods in engineering, 45(5) (1999) 601-620.

[27] N. Moës, J. Dolbow, T. Belytschko, A finite element method for crack growth without remeshing, International journal for numerical methods in engineering, 46(1) (1999) 131-150.

[28] J.E. Dolbow, An extended finite element method with discontinuous enrichment for applied mechanics, Northwestern university, 1999.

[29] N. Sukumar, N. Moës, B. Moran, T. Belytschko, Extended finite element method for three-dimensional crack modelling, International journal for numerical methods in engineering, 48(11) (2000) 1549-1570.

[30] M. Stolarska, D.L. Chopp, N. Moës, T. Belytschko, Modelling crack growth by level sets in the extended finite element method, International journal for numerical methods in Engineering, 51(8) (2001) 943-960.

[31] S. Mohammadi, Extended finite element method: for fracture analysis of structures, John Wiley & Sons, 2008.

[32] B. Bourdin, G.A. Francfort, J.-J. Marigo, Numerical experiments in revisited brittle fracture, Journal of the Mechanics and Physics of Solids, 48(4) (2000) 797-826.

[33] W. Lv, B. Ding, K. Zhang, T. Qin, High-Cycle Fatigue Crack Growth in T-Shaped Tubular Joints Based on Extended Finite Element Method, Buildings, 13(11) (2023) 2722.

[34] S. Bhattacharya, I.V. Singh, B. Mishra, Mixed-mode fatigue crack growth analysis of functionally graded materials by XFEM, International Journal of Fracture, 183 (2013) 81-97.

[35] K. Hasikin, N. Soin, F. Ibrahim, Modeling an optical diaphragm for human pulse pressure detection, in: WSEAS International Conference. Proceedings. Mathematics and Computers in Science and Engineering, World Scientific and Engineering Academy and Society, 2009.

[36] G.D. Quinn, J. Salem, I. Bar-On, K. Cho, M. Foley, H. Fang, Fracture toughness of advanced ceramics at room temperature, Journal of research of the National Institute of Standards and Technology, 97(5) (1992) 579.